geosciences

MDPI

Article

Damage to Churches after the 2016 Central Italy Seismic Sequence

Barbara Ferracuti [1], Stefania Imperatore [1], Maria Zucconi [1,*] and Silvia Colonna [2]

[1] Department of Civil Engineering, "Niccolò Cusano" University, Via Don Carlo Gnocchi, 3, 00166 Rome, Italy; barbara.ferracuti@unicusano.it (B.F.); stefania.imperatore@unicusano.it (S.I.)
[2] Comune di Polignano a Mare, Viale delle Rimembranze 21, 70044 Polignano a Mare, Italy; silviacolonna@comune.polignanoamare.ba.it
* Correspondence: maria.zucconi@unicusano.it

Abstract: The present study focuses on seismic damage to 36 masonry churches observed after the 2016 Central Italy earthquake. In the sample, recurrent architectural and structural features were identified and accurately described. In order to classify the churches in the sample based on their safety level, their seismic vulnerability was assessed by adopting the simplified procedure proposed in the current Italian standards for cultural heritage. The observed damage, directly detected by the authors during the post-earthquake surveys, is presented and carefully described, highlighting the evolution of the damage. An analysis of the damage suffered by the inspected churches highlighted the most frequent causal mechanisms and the most vulnerable macroelements. Particular attention was devoted to computation of a damage index based on the observed damage as well as on the macroelements present in the surveyed churches. Moreover, a judgment of usability, i.e., whether a church could be occupied after a seismic event, was made using the official survey form and related to both the seismic intensity experienced and the observed damage index. An analysis of the collected data enabled consideration of the usability judgment with respect to the damage index values, computed according to the Italian standards.

Keywords: 2016 Central Italy earthquake; churches; post-seismic surveys; observed damage

Citation: Ferracuti, B.; Imperatore, S.; Zucconi, M.; Colonna, S. Damage to Churches after the 2016 Central Italy Seismic Sequence. *Geosciences* **2022**, *12*, 122. https://doi.org/10.3390/geosciences12030122

Academic Editors: Sabina Porfido and Jesus Martinez-Frias

Received: 7 January 2022
Accepted: 28 February 2022
Published: 4 March 2022

1. Introduction

Italy is an earthquake-prone country; several seismogenic areas are located in Italian territory, and the central–southern Apennines chain has generated strong earthquakes in Italy throughout history [1–4]. Over the years, post-earthquake damage observation has highlighted the significant seismic risk to historical towns [5–12], with respect to both ordinary buildings [13–17] and historical constructions [18–27]. The high vulnerability of the cultural heritage has been confirmed by post-earthquake usability inspections organized by the Civil Protection Department. After the 2009 L'Aquila earthquake, only 23.3% of inspected monuments remained usable, in contrast to 52.6% of ordinary buildings [28]; similar outcomes were detected after the Central Italy earthquake [29].

The seismic performance of historical masonry constructions is influenced by an insufficient connection between horizontal and vertical bearing elements; a crack pattern subdivides the structure into distinct macroelements with autonomous behavior, such that box behavior cannot occur [30–32]. Due to the architectural feature particular to churches, such as large halls, slender walls, lack of intermediate horizontal floors, and heavy, thrusting structures—such as domes and vaults—local collapse mechanisms are emphasized. Analysis of the damage occurring after the most significant Italian earthquakes (Friuli, 1976; Irpinia, 1980; Umbria–Marche, 1997; Molise, 2002; L'Aquila, 2009; Emilia, 2012) highlighted that the seismic performance of masonry churches was governed by the autonomous responses of single architectural portions [33–36], and the related damage depended on both their architectural morphology and their construction details [37,38]. Both these features vary from country to country and from region to region. Nevertheless,

the most frequently damaged macroelements can be identified. According to damage analyses systematically carried out after recent earthquakes (e.g., Italy from 2009 to 2017; Chile, 2010; New Zealand, 2010–2011; Mexico, 2017), the most recurrent mechanisms involved façades, rooves, apses, vaults, and belltowers [39–48].

From August 2016, a seismic sequence characterized by medium–high magnitudes involved the Central Italy Apennines. The earthquake caused serious economic losses and a great number of casualties (303 deaths). Several municipalities, including Amatrice, Accumoli, Arquata, Norcia, and Visso, registered severe damage to existing building stocks, especially to unreinforced masonry buildings and historical constructions, mainly where significant seismic provisions were missing. About 65,500 ground motions were attributed to the same seismic sequence (3500 with $M_w \geq 2.5$). The mainshock ($M_w = 6.0$) was registered on 24 August, with the epicenter in Accumuli, and caused destruction of Amatrice. A further earthquake, of $M_w = 5.90$ and with its epicenter in the town of Ussita, occurred on 26 October. The strongest ground motion was recorded on 30 October near the municipality of Norcia, characterized by $M_w = 6.5$, when the collapse of the Basilica of San Benedetto in Norcia occurred. This last event was the strongest earthquake since that occurring in Irpinia in 1980. Finally, on 18 January, three further significant earthquakes with M_w between 5.1 and 5.5 were registered in the southern sector of the sequence [49–55].

The effects of the 2016–2017 Central Italy seismic sequence on historical masonry churches have been thoroughly investigated over the past three years, as teams of experts from several Italian academic institutions were engaged to assess the damage that had occurred, evaluating building usability as well as recommending immediate provisional interventions. These activities were promoted by the Italian Ministry of Cultural Heritage (MiBACT) and coordinated by the Italian Civil Protection Department (DPC) through its competence center, the ReLUIS (Laboratories University Network of Seismic Engineering) consortium. The activities carried out in the post-earthquake emergency phase were described in [56]. Damage surveys of historical and monumental buildings, and of churches, started on 13 September 2016, under the supervision of MiBACT officials, experts in the cultural heritage of the territories affected by the Central Italy seismic sequence. The main purposes of the inspections were the following: (i) to perform damage surveys of cultural heritage buildings and their resulting safety level; (ii) to identify emergency measures necessary to guarantee public safety, as well as to limit worsening of structural conditions under static and dynamic stresses; and (iii) to safeguard valuable movable objects, i.e., paintings and statues. The damage survey forms for cultural heritage buildings, i.e., churches [57] and palazzi [58], were filled in according to instructions issued by MiBACT for safe activity management and cultural heritage protection in emergencies arising from natural disasters [59]. A report of the survey activities undertaken on churches, together with a summary of the usability outcomes and preliminary observations on damage, can be found in [60].

Research studies into the performance of historical masonry churches affected by the Central Italy earthquakes can be divided into two macro-categories. The first group of papers [61–68] present case studies in which damage suffered and collapses are carefully described, with back-analyses of surveyed damage performed, including employment of sophisticated numerical methods. The amount of detail describing the surveyed damages is progressively reduced, increasing the complexity of analyses. Certain studies (e.g., [61–63]) evaluate the seismic behavior of a single church by means of conventional analyses and linear numerical models, performing damage assessment through technologically advanced instruments, such as unmanned aerial vehicle (UAV) image sequencing and use of the UAV 3D model. Some studies (e.g., [64–66]) present detailed 3D FEM models (also nonlinear), describing earthquake damage by means of photographic surveys coupled to evaluation of crack pattern relief. Further studies [67–69] report complex nonlinear analyses on several churches, describing the main damage that occurred.

Since in [61–69], the main aim was assessment of churches' seismic vulnerability, data later collected in post-earthquake survey forms was never considered. In contrast, a

considerable amount of observed data extracted from survey forms was collected in the second group of papers [70–75], focusing on the development of predictive models for the seismic damage of historical churches, also by means of complex methodologies. The first paper defining empirical fragility curves for masonry churches was proposed by Hofer et al. [70], who collected 196 survey forms of churches with the aim of deriving fragility curves based on the observed mean global damage index, and with the aim of identifying the structural peculiarities of Italian "Apennine churches". Subsequently, De Matteis and Zizi [71,72] estimated the vulnerability indexes of a homogeneous sample of 68 one-nave churches according to the simplified approach proposed by the Italian guidelines [76]. Moreover, in [71,72], observed damage was compared to the values estimated through the predictive function proposed in [36], and a revised formulation for the expected average damage based on the peak ground acceleration (*PGA*) instead of the macroseismic intensity level (I_{MCS}) was proposed. Canuti et al. [73] considered a sample of 514 churches for computing damage probability matrices with respect to both the global damage index and the single mechanism. The churches' vulnerability indexes were finally derived by introducing the observed mean global damage index in the model of observational vulnerability proposed in [36]. Cescatti et al. [74] performed a statistical analysis of 889 inspections to assess the main seismic vulnerabilities of churches in Central Italy. The deep analysis of the survey's forms highlighted that most of Central Italian religious buildings are simple (one-nave churches with or without apse), as was also remarked in [70]. Therefore, based on such homogeneous vulnerability, and using data from a class composed of 633 churches, damage probability matrices were defined for different damage levels, and empirical fragility curves were derived. Finally, Morici et al. [75] statistically processed the damages of 514 religious buildings belonging to the Archdiocese of Camerino–San Severino, with the main aim of deriving the expected damage scenarios for the Marche region.

In the present paper, the damages of 36 churches during the 2016 Central Italy earthquake are presented. After a brief description of the historical and architectural features of the inspected churches, their vulnerability was assessed according to the simplified procedure of the Italian standards, as proposed in [76]. Then, the global damage index, based on the observed damage collected during the surveys, was evaluated, according to [57,76]. The dependence of the observed damage by the seismic intensity suffered by the churches was investigated considering both peak ground acceleration (*PGA*) and macroseismic intensity (I_{MCS}) as seismic intensity measures. Finally, the damage index was compared with the usability judgment for each inspected church and some drawbacks on the definition of the damage index are shown.

2. Inspected Churches

After an earthquake, the post-emergency Civil Protection Department activities include the identification of the most stricken and damaged areas—the "red zones"—and the evaluation of the structural safety of the damaged buildings. This knowledge is necessary to ensure the safety of the people involved in the seismic event. The architectural heritage is also analyzed in the post-emergency stage, with the following primary aims: (i) evaluating the usability of the buildings; (ii) implementing provisional measures to ensure the safety of citizens and users; (iii) drawing up a priority of the provisional safety operations; (iv) preserving the pieces of art which are in danger; (v) estimating realistic levels of national funding for the reconstruction phase.

After the 2016 Central Italy earthquakes, the authors, as ReLUIS members, participated in the activities surveying monumental buildings, which were coordinated by the Italian Civil Protection Department and the Ministry of Cultural Heritage. In this framework, a total of 36 churches were inspected starting from September 17: 11 were in the municipalities of Accumoli and Amatrice (near the epicenter of 24 August); 20 were near the city of Teramo (approximately 40 km away from the 24 August epicenter); the 5 farthest away are located near Macerata, in the northern surveyed area, or in the proximity of L'Aquila

city (at about 80 km from the epicenter of 30 October). The geographical localization of the inspected churches is represented in Figure 1a, while in Figure 1b, as an example, an image of a collapsed church observed during the inspection in the Amatrice municipality is shown.

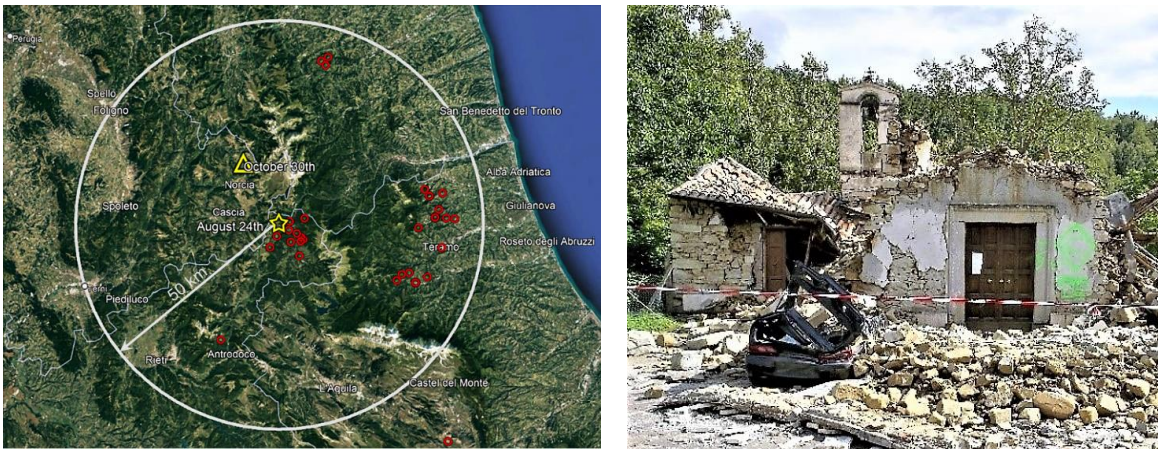

(**a**) (**b**)

Figure 1. (**a**) Geographical localization (adapted from Google Earth) of the inspected churches (red circles), with the position of epicenters of 24 August (yellow star) and 30 October 2016 (yellow triangle); (**b**) a disrupted church in Amatrice, 5 km away from the epicenter of 24 August.

All the examined monuments belong to the Italian Cultural Heritage, representing tremendous cultural and sociological value for the inhabitants of the localities and for history. The largest number of surveyed churches was founded in the XV–XVI century, as is the case of the Dome in Campli (Figure 2a). The oldest surveyed church is the Romanic Abbey of Holy Mary in Montesanto near Teramo (Figure 2b), which—according to the popular tradition—was founded in the VI century AD by Saint Benedict from Norcia. Contrarily, historical sources suggest that the Abbey was founded during the XI century, becoming one of the most powerful Benedictine Monasteries of the region in the medieval period. The following sections briefly analyze the surveyed churches in terms of historical features, plan configuration, and masonry quality. A simplified vulnerability assessment was carried out according to the Italian guidelines provisions on the assessment and the mitigation of seismic risk on cultural heritage [76].

(**a**) (**b**)

Figure 2. Two examples of surveyed churches: (**a**) Holy Mary in Platea in Campli, Teramo (XV Cen.); (**b**) Abbey of Holy Mary in Montesanto in Teramo (X–XI Cen.).

2.1. Historical and Architectural Features

The investigated churches were founded in five distinct temporal–architectonic intervals (Figure 3a). In detail, 22.22% of the sample is composed of medieval churches, characterized by poor decoration, in accordance with the main peculiarity of Central Italian medieval churches [77,78]. A proportion of 29.17% of the inspected churches were founded between the XV and the XVI centuries (the Renaissance period), including the meaningful example of the Dome in Campli (Figure 2a). The religious buildings belonging to the Baroque period (from the XVI to the XVII century) are characterized by impressive facades, with interiors animated by aisles, vaults, and often rich frescoes—such churches constitute 26.39% of the sample. The architecture of the Neoclassical cluster (12.50% of the sample) is inspired by Classical Era principles; therefore, the spatial characterization is marked by stuccoes, producing a well-balanced dynamism that never exhibits contrasting tensions. The last set (9.72% of the sample) was built in the Modern Age, i.e., in the XX century, and it is composed of churches of smaller dimensions and often characterized by less refined masonry (irregular texture characterized by stone elements).

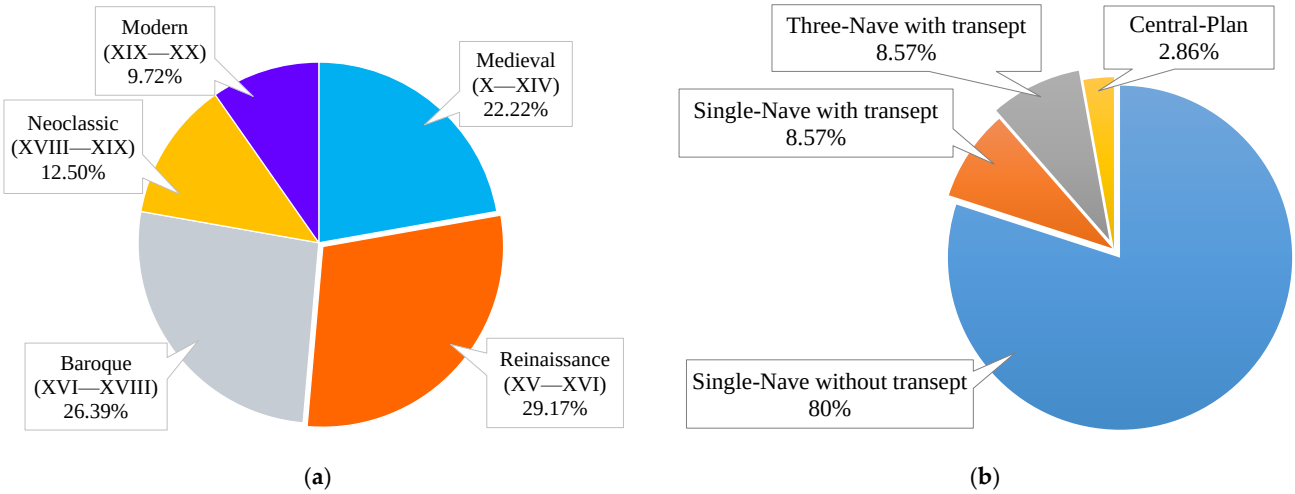

Figure 3. Foundation period of the surveyed churches (**a**) and architectural features (**b**).

Among the different architectural key features, the main distinction that characterized the seismic response is the plan configuration according to the approach already adopted by other authors [21–23,43,60,70–75]. According to the characteristics of the surveyed churches, the considered layouts comprise the following: single-nave typology (SN), one nave with transept (SNT), three naves and transept (3NT), and central plan configuration (C). It can be observed that the single nave configuration, that of SN and SNT, is the most frequent layout, while only 12% of the sample presents a more complex architectural conformation (Figure 4a). Such results are in line with the remarks of other authors [70,74]. In Figure 4, some examples of inspected churches with different plan configurations are reported.

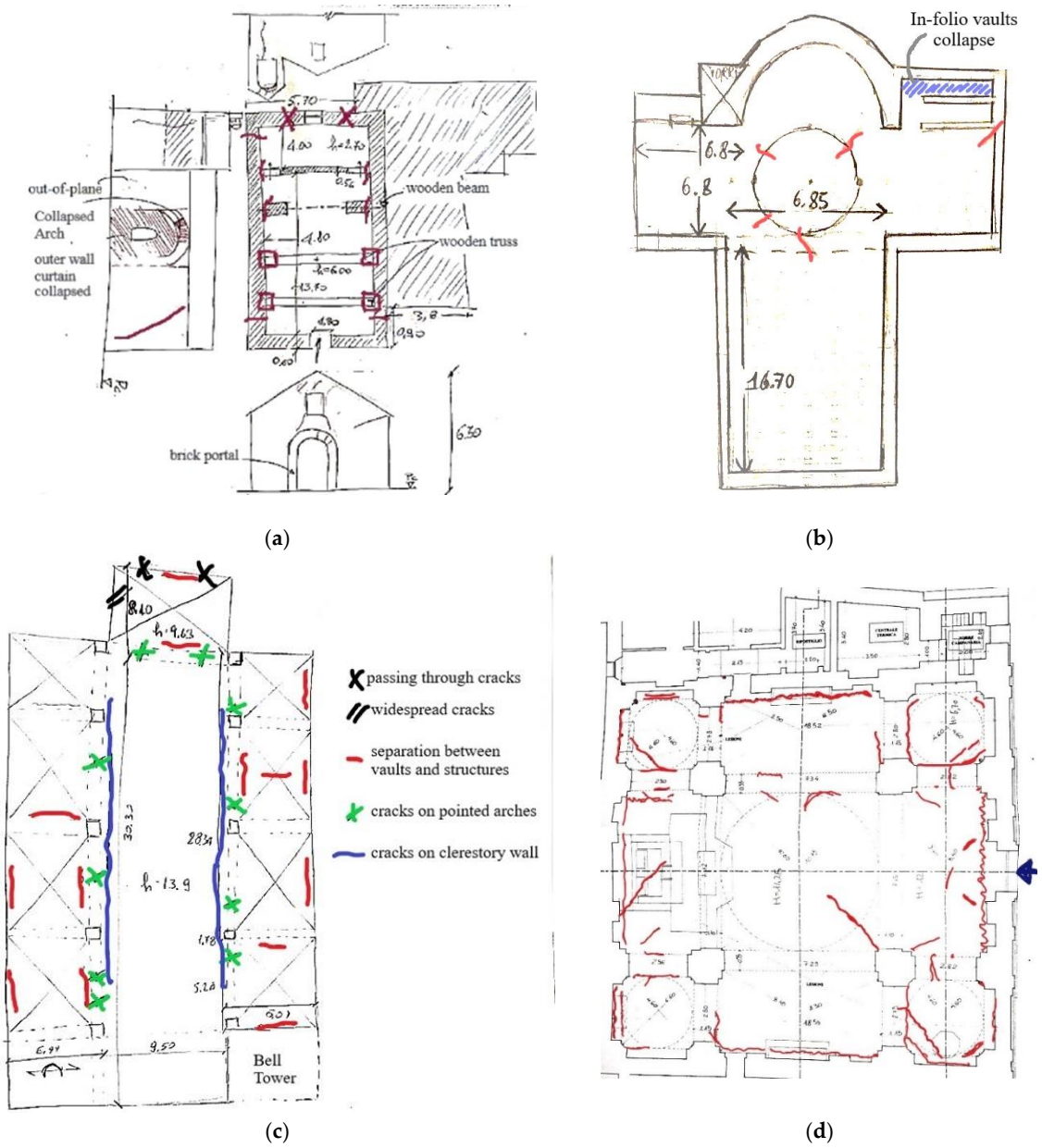

Figure 4. Plan configuration with observed crack patterns of some inspected churches: sketches made during the inspections. (**a**) Single nave (SN) typology: the church of Saint Elpidio in Campli. (**b**) One nave with transept (SNT): St. Lowrance in Civitella del Tronto. (**c**) Three naves and transept (3NT): the Dome of Campli, Holy Mary in Platea. (**d**) Central plan configuration (C): the church of Saint Savino in Gualdo.

To summarize, the single nave without transept (SN) category comprises the larger sample, i.e., 80% of the inspected churches. Among them, 27.59% were built in the Medieval era, 24.14% in the Renaissance, and 20.69% in the Neoclassical period. The churches characterized by a single nave and built in the Baroque or Modern period comprise 13.79% of the clusters in both cases. All the churches characterized by the single nave without transept are moreover characterized by the following features: (i) a façade with a rose window over the entrance and a triangular or rectangular gable; (ii) a double pitched timber roof; (iii) a belltower beside the church. These typical features depict the "Apennine church" typology, as defined in [44,67,70,74] after the Central Italy earthquake. An example of a surveyed "Apennine church" is the St. Maxim Oratory in Collalto (Amatrice), sketched in Figure 5.

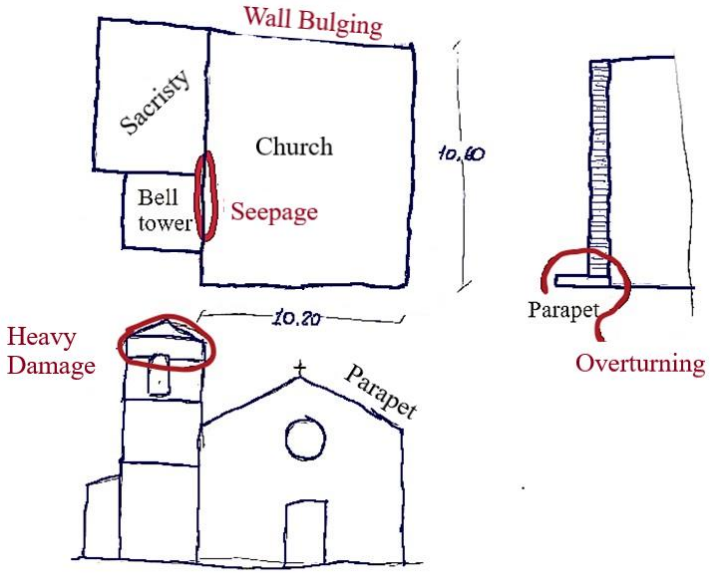

Figure 5. Typical architectural features of the "Apennine church": the case of the St. Maxim Oratory in Collalto, Amatrice. Sketches made during the inspections.

2.2. Structural Features

The inspected churches are characterized by different masonry typologies, depending on their geographic location and the importance attributed to the church by the community (Figure 6). The typical masonry walls often consist of local irregular stones, frequently characterized by a double layer and a poor-quality mortar (Figure 6a), as also observed by other authors analyzing the churches stricken by the Central Italy earthquake [74]. In the case of medium-importance structures, i.e., St. Savino in Gualdo, the prevailing availability of irregular calcareous stones result in a medium-quality wall (Figure 6b); however, in the case of seismic action, it could easily crumble. Among the surveyed churches, the cases of good-quality masonry are rare and observed only in important monuments, i.e., the Abbey of Holy Mary in Montesanto, in which calcareous bricks, regular in size and shape, can be observed (Figure 6c).

(**a**) (**b**) (**c**)

Figure 6. Different masonry typologies surveyed: (**a**) typical double-layer wall without headers (St. Francis, Amatrice); (**b**) irregular rubble masonry with partially staggered vertical joints (St. Savino in Gualdo, Macerata); (**c**) calcareous squared stones masonry (Abbey of Holy Mary in Montesanto, Civitella del Tronto).

Several churches present domes (Figure 7) and vaults (Figure 8), among these, the false camorcanna vaults (Figure 8a) and the more vulnerable in folio vaults (Figure 8b) were observed. In the case of inspectable roofing, a non-pushing timber light roof was typically

detected (47% of the sample); only in one church—the Virgin of Rescue in Campli—was the gable roof made of one-way ribbed slab.

(**a**) (**b**)

Figure 7. Surveyed domes: (**a**) St. Lowrance in Civitella del Tronto; (**b**) St. Savino in Gualdo, Macerata. The observed crack pattern has been highlighted in red.

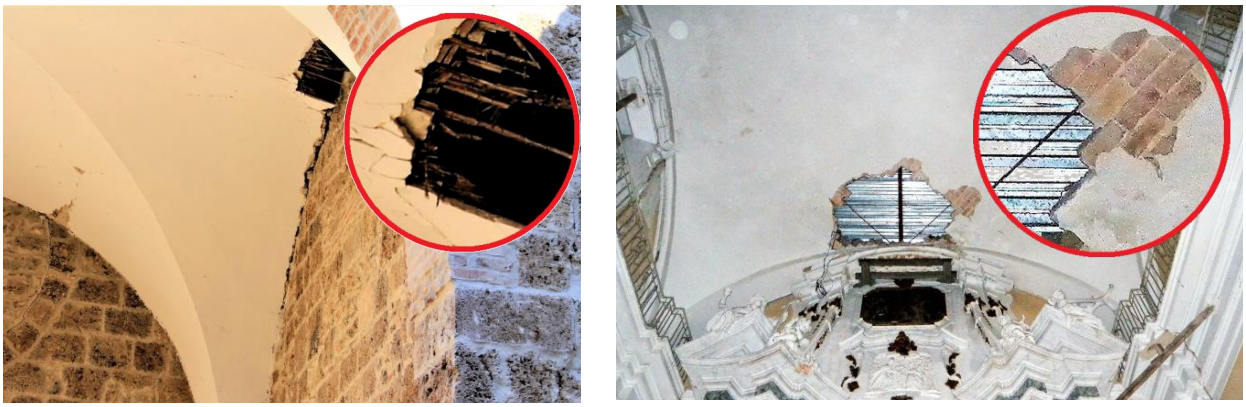

(**a**) (**b**)

Figure 8. Surveyed vaults: (**a**) the false camorcanna vaults of Abbey of Holy Mary in Montesanto, Civitella del Tronto; (**b**) the in folio vaults of St. Anthony Abbot in Teramo.

2.3. Simplified Vulnerability Assessment

In order to evaluate whether the church sample was composed of homogenous data in terms of structural features and seismic responses, the surveyed churches' vulnerability was assessed according to the simplified LV1 procedure proposed by the Italian guidelines on the assessment and the mitigation of the seismic risk on the cultural heritage [76]. The methodology analyses the constructive details and features according to the procedure proposed in [36], through the direct observation of the existing macroelements, including 28 mechanisms (M), as shown in Table 1. The principal advantage of the approach is the limited amount of data necessary, which is essential for a quick assessment. The LV1 methodology allows having a first seismic vulnerability classification of the church based on the assessment of a vulnerability index that ranges from 0 (if the church does not present seismic vulnerability) to 1 (if the church has a high vulnerability). The vulnerability index, i_v, is defined as a weighted sum of the vulnerability indicator assigned to all possible local mechanisms that could occur in the structure, regardless of the probability of their

contemporary activation. According to [76], the vulnerability index can be estimated as follows:

$$i_v = \frac{1}{6} \times \frac{\sum_{k=1}^{28} \rho_k \times \left(v_{ki} - v_{kp}\right)}{\sum_{k=1}^{28} \rho_k} + \frac{1}{2} \quad (1)$$

where v_{ki} is the indicator of vulnerability attributed to the k-th mechanism associated with a specific macroelement, and v_{kp} is the indicator of vulnerability assigned to the seismic protection devices of the same mechanism (i.e., tie rods, buttresses, etc.). Both these indicators vary between 0 and 3 and are evaluated according to an expert's judgment: v_{ki} increases with the vulnerability of the macroelement, and v_{kp} increases with the effectiveness of the seismic protection device. Therefore, v_{ki} = 0 means that the kinematic mechanism cannot be activated (i.e., the macroelement is absent), while v_{kp} = 0 means that the aseismic protection devices are ineffective or absent. On the contrary, the value 3 is assumed for highly vulnerable macroelements or when the devices can inhibit the associated kinematic mechanisms.

Table 1. Possible mechanisms considered for each macroelement of the church.

Macroelement	Collapse/Damage Mechanism	ID	ρ_k
Façade	Overturning of the facade	M1	1.0
	Damage at the top of façade (gable)	M2	1.0
	Shear mechanisms in the façade	M3	1.0
-	Narthex	M4	0.5
Nave	Transversal vibration of the nave	M5	1.0
	Shear mechanisms in the side walls	M6	1.0
	Longitudinal response of the colonnade	M7	1.0
Vaults	Vaults of the nave	M8	1.0
	Vaults of the aisles	M9	1.0
	Vaults of the transept	M12	0.5–1.0
	Vaults in presbytery and apse	M18	0.5–1.0
Transept	Overturning of the transept's end wall	M10	0.5–1.0
	Shear mechanisms in the transept walls	M11	0.5–1.0
Triumphal arch	Triumphal arches	M13	1.0
Dome	Dome and lantern	M14	1.0
	Lantern	M15	0.5
Apse	Overturning of apse	M16	1.0
	Shear mechanisms in presbytery and apse	M17	1.0
Roof	Roof mechanisms: side walls of nave and aisles	M19	1.0
	Roof mechanisms: transept	M20	0.5–1.0
	Roof mechanisms: apse and presbytery	M21	1.0
Chapel	Overturning of the chapels	M22	0.5–1.0
	Shear mechanisms in the walls of chapels	M23	0.5–1.0
	Vaults of chapels	M24	0.5–1.0
-	Interactions next to irregularities	M25	0.5–1.0
	Projections (domed vaults, pinnacles, statues)	M26	0.5–1.0
Belltower	Belltower	M27	1.0
	Belfry	M28	1.0

For all the analyzed churches, the obtained vulnerability indexes are listed in Table 2 and reported in Figure 9. It is worth underlining that the vulnerability index cannot be evaluated for the collapsed churches (C12, C26–C29), since the inspections were realized only after the earthquake when the collapses had occurred. The results of the LV1 procedure (Table 2, Figure 9) show a predominant low–medium vulnerability of the inspected churches: 39% of the sample is characterized by a low vulnerability index (lower or equal

to 0.40), 36% had medium vulnerability (the vulnerability index ranges between 0.40 and 0.60), and 25% were marked by high vulnerability.

Table 2. Inspected churches list: Location, name, identification number (ID), and vulnerability index (i_v) evaluated according to the LV1 approach.

Place	Church	ID	i_v
Micigliano (Rieti)	Abbey St. Quirico and St. Giulitta	C1	0.22
Case Vernesi (Montorio, Teramo)	St. Andrew	C2	0.22
Altavilla (Montorio, Teramo)	St. Andrew Apostle	C3	0.24
Pagannoni (Campli, Teramo)	St. Peter in Pensilis	C4	0.32
Gualdo (Macerata)	St. Peter	C5	0.35
Teramo	St. Anthony Abbot	C6	0.48
Fichieri (Campli, Teramo)	Virgin of Rescue	C7	0.64
Collalto (Amatrice, Rieti)	Oratory St. Maxim	C8	0.39
Gualdo (Macerata)	St. Elpidio	C9	0.73
Cornillo Vecchio (Amatrice, Rieti)	St. Francis	C10	0.77
Cossito (Amatrice, Rieti)	Annunciation	C11	0.96
Casale (Amatrice, Rieti)	Virgin of Carmine	C12	Collapsed
Civitella del Tronto (Teramo)	St. Francis	C13	0.29
Campli (Teramo)	Immaculate Conception	C14	0.21
Montorio (Teramo)	St. Rocco	C15	0.38
Navelli (L'Aquila)	Holy Mary of Rosary	C16	0.48
Pagannoni (Campli, Teramo)	St. Peter in Pensilis	C17	0.35
Montorio (Teramo)	Holy Mary of Mercy	C18	0.36
Rojano (Campli, Teramo)	Holy Mary ad Venales	C19	0.39
Montorio (Teramo)	St. Sebastian	C20	0.37
Poggio d'Api (Accumoli, Rieti)	Holy Mary of Piano	C21	0.38
Campli (Teramo)	St. Paul	C22	0.56
Campli (Teramo)	St. Francis	C23	0.49
Civitella del Tronto (Teramo)	Holy Mary in Montesanto	C24	0.54
Roccasalli (Accumoli, Rieti)	St. Giovenale	C25	0.56
Tino (Accumoli, Rieti)	Annunziata Church	C26	Collapsed
Macchia (Accumoli, Rieti)	St. Peter and St. Paul	C27	Collapsed
Poggio Casoli (Accumoli, Rieti)	St. Lucia	C28	Collapsed
Accumoli (Rieti)	St. Lawrence and St. Paul	C29	Collapsed
Civitella del Tronto (Teramo)	St. Flavian	C30	0.44
Boceto (Campli, Teramo)	Holy Mary Assumpted	C31	0.56
Civitella del Tronto (Teramo)	St. Lawrence	C32	0.55
Montorio (Teramo)	Sanctuary Holy Mary of Sgrima	C33	0.46
Campli (Teramo)	Dome Holy Mary in Platea	C34	0.44
Terracino (Accumoli, Rieti)	St. George	C35	0.59
Gualdo (Macerata)	St. Savino	C36	0.60

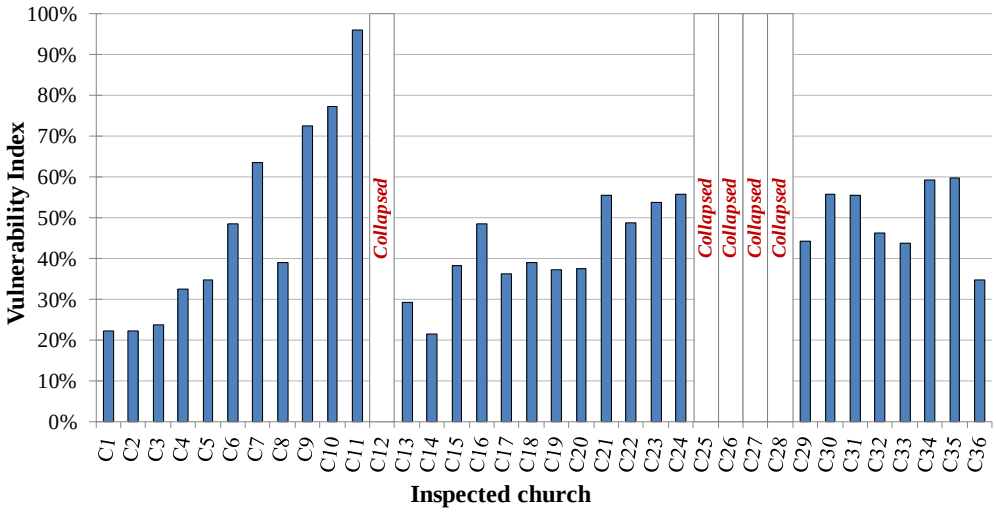

Figure 9. Vulnerability index evaluated for the inspected churches according to the LV1 approach.

It is worth noting that the attained vulnerability index could not be fully representative of the effective seismic vulnerability of the church, although the score assigned to the indicators of vulnerability is a key factor for the final assessment of i_v. In fact, the church vulnerability is strictly related to the vulnerability of the most relevant macroelements (facade, elements of the nave or the apse, triumphal arches, and belltower), as well as being reliant on the occurrence of activation of the related kinematic mechanism. Instead, the vulnerability index evaluated according to the LV1 approach disregards proper coefficients of combination to consider the non-simultaneous triggering of the kinematic mechanisms. Consequently, the vulnerability index perceives the possibility of contemporary activation of all possible mechanisms, even if distinct macroelements can independently move and collapse when an earthquake shakes an ancient masonry church.

Although each element should be properly weighted to account for their different rule in the seismic response, according to [76], almost all macroelements are considered of equal importance; therefore, the weight affects the final value of i_v only in a limited way. In this perspective, the LV1 approach was recently criticized [77,78], and a more flexible definition of the adopted weights was suggested.

3. Observed Damages

The earthquake which occurred on 30 October 2016 was the strongest Italian seismic event in the last 40 years [79]: the event, with an epicenter located 5 km away from the municipality of Norcia, recorded 6.5 magnitude. The shock was a part of a wider sequence, called "Central Italy Earthquake 2016", and started on 24 August with a first earthquake of 6.0 magnitude and an epicenter near the municipality of Accumoli.

In the survey activities promoted by the Civil Protection Department and the Italian Cultural Heritage Ministry, the authors directly observed the damages caused by the two mainshocks of 24 August and 30 October. According to the lessons from the Friuli earthquake and the Emilia-Romagna earthquake [42], the cumulative damages in the Central Italy earthquake were significant and, in several cases, dramatic. Evidence of the damage evolution due to multiple seismic events is represented in Figure 10, where the evolution of damage in the St. Lawrence and St. Paul Church in Accumoli (C29) is depicted: the shock, which occurred on the 24 August, activated the rocking motion of the gable of the façade up to its collapse (Figure 10b); then, when the shock of the 30 October occurred, the church totally disintegrated (Figure 10c).

(**a**) (**b**) (**c**)

Figure 10. The St. Lawrence and St. Paul Church in Accumoli: (**a**) before the Central Italy earthquake; (**b**) after the 24 August strong motion; and (**c**) after the earthquake occurred on 30 October 2016.

Upon the first examination, the more recurrent damages suffered by the inspected "Apennine church", i.e., the typical religious building typology in the analyzed geographical context, concern the façade. As also remarked by several authors, based on the collected aftershock data analysis [21–23,34,42,44,47,48,74], the façade is the most frequently damaged macroelement, and the overturning is the most dangerous mechanism. Analogously, the crack patterns observed in the St. Francis Church in Amatrice (C10), before and after the 24 August shock, evidence that the damages mainly struck the façade macroelement (Figure 11a,b). The results of the St. Peter and St. Paul Church inspections in Accumoli (C27) point out the same evidence of this out-of-plane mechanism (Figure 12a,b). It is worth noting that if the connection between the wall leaves is poor, as in the case of the St. Elpidio church in Gualdo (C9, Figure 13), where an opening under the arch was closed by a poor-quality masonry wall, and the out-of-plane mechanism appears as a detachment of the external masonry layer, since the masonry does not express any monolithic behavior. Therefore, a wall can experience a partial disruption for seismic acceleration values lower than the one corresponding to the activation of the kinematic motion of the entire wall.

With specific reference to the out-of-plane motion of the façade, it is worth noting that the 2016 Central Italy earthquake presents a strong directionality, as suggested by the acceleration response spectra of the two main events (Figure 14). In particular, the higher seismic acceleration struck the region in the east–west direction, corresponding to the so-called "sacred direction" of the churches (east–west axis), until the II Vatican Council (1960). As an explanatory case, the example of the Saint George Church in Terracino (C35) is given, for which the overturning mechanism of the façade is evident (Figure 15).

Aside from the façade mechanism, the overturning mechanism causes the abrupt displacement of the imposts of arches and vaults or domes; these structures, frequently made with bricks arranged in folio, can easily move into the minimum thrust condition, and then collapse, as in the example of St. Savino church in Gualdo (C36, Figure 16).

(**a**) (**b**)

Figure 11. The St. Francis church in Cornillo Vecchio (Amatrice): (**a**) before and (**b**) after the earthquake occurred on 24 August 2016.

(**a**) (**b**)

Figure 12. The St. Peter and Paul church in Macchia (Accumoli), before (**a**) and after (**b**) the earthquake occurred on 30 October 2016.

(**a**) (**b**)

Figure 13. Disruption of the masonry leaf due to the out-of-plane behavior in the St. Elpidio church in Gualdo, Macerata: (**a**) external and (**b**) internal views.

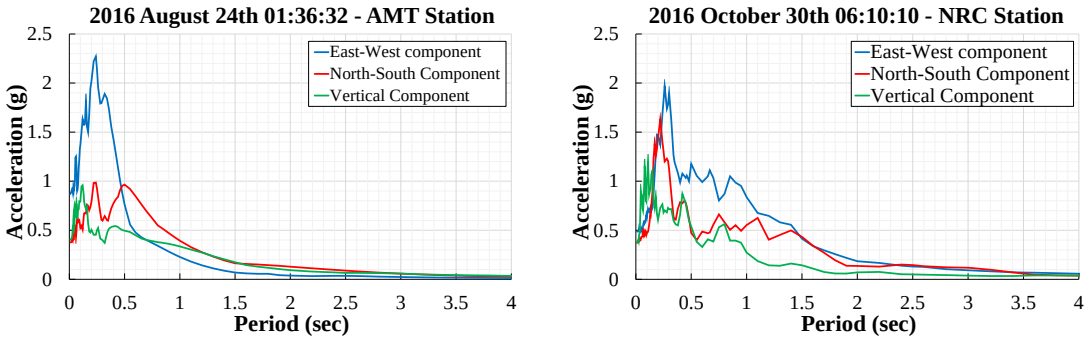

(**a**) (**b**)

Figure 14. Acceleration response spectra for the 24 August (**a**) and 30 October (**b**) main shocks [80].

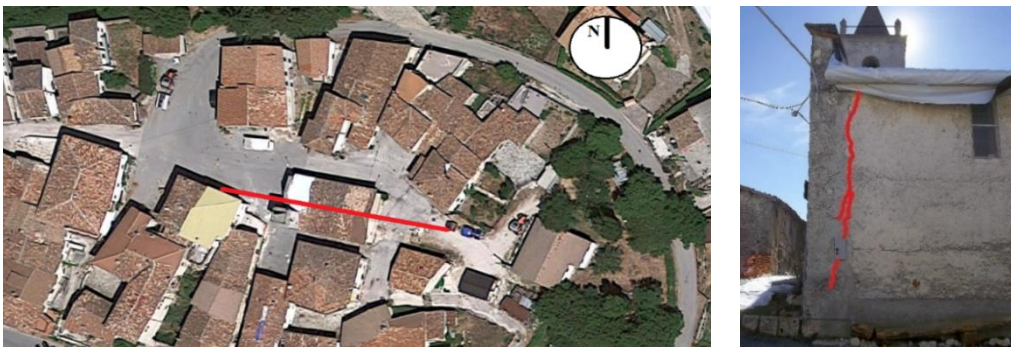

(**a**) (**b**)

Figure 15. St. George church in Terracino (Accumoli): (**a**) aerial photography (adapted from Google Maps) with east–west axis orientation (red line); (**b**) façade overturning mechanism (cracks emphasized in red).

(**a**) (**b**)

Figure 16. The dome in St. Savino church in Gualdo, before (**a**) and after (**b**) the earthquake occurred on 30 October 2016.

The clerestory walls, typically present in three naves churches, are characterized by a high vulnerability to out-of-plane action. These structural elements correspond to the short walls of the central nave located above the arches separating the central nave from the lateral nave. Since they should support only the weight of the roof structures, the clerestory

walls are typically slenderer than the other walls; moreover, they are often marked by full-height windows, allowing the appropriate brightness for the religious building. Both these aspects, coupled to the vertical amplification of seismic motion, promote the formation of splitting cracks spreading on the top and lower sections of the element, as observed in the example of the Dome of Campli (C34, Figure 17). It is interesting to recall that similar damages were recorded after the Emilia earthquake [42].

Figure 17. Out-of-plane of the clerestory wall in Holy Mary in Platea in Campli, Teramo.

The belltowers frequently present damages in the pinnacles, in the bell cell, and along the tower. In particular, the damage on the stem can be detected when the variation of the vertical stiffness in the structure is significant, i.e., for towers connected to the church (Figure 18). Instead, the most damaged element becomes the cell when the variation in stiffness is more gradual. In fact, in all inspected cases these elements are characterized by the presence of large openings and by vertical bearing elements with reduced thickness, since the working loads that they should sustain are low. Consequently, the cells can experience a shear failure, as in the case of the St. Savino church in Gualdo (C36), where a significant crack pattern on the piers was detected (Figure 19a). Finally, when the piers are strong enough, the damages are localized on the upper part of the cell (Figure 19b).

(**a**) (**b**)

Figure 18. Damages on the stem of the belltower (**a**,**b**): the case of the St. Francis church in Campli (C23). The observed crack pattern has been highlighted in red.

(**a**) (**b**)

Figure 19. The structural component of the bell cell: (**a**) the case of St. Savino church in Gualdo (C36); (**b**) the case St. Maxim Oratory in Collalto, Amatrice (C8).

Among the mechanisms frequently detected in the post-seismic survey activities, the in-plane shear mechanism in the façade or in the lateral walls (Figure 20a) and the roof cover mechanism with the sliding of the timber beams (Figure 20b) must be mentioned. This mechanism could be very dangerous due to the possible loss of the support for the timber beams with the consequent roof collapse.

(**a**) (**b**)

Figure 20. Other mechanisms activated in the wall: (**a**) shear mechanism in the lateral walls in St. Giovenale church in Roccasalli (C25); (**b**) roof covering mechanism in in St. Elpidio church in Campli (C9).

3.1. Possible and Activated Collapse Mechanisms

In this section, a synthesis related to the possible and the activated mechanisms observed during the inspection is given for the 36 Apennine churches inspected by the authors after the Central Italy earthquake. Specifically, during the surveys, the first point was to identify whether the macroelement was present in the church, and then, if present, to identify whether it was damaged.

Figure 21 shows the relative presence and occurrence of the mechanism activation for each macroelement—recalled following the nomenclature used in Table 1. Observing the red bars, in more than 90% of the surveyed churches the façade, (M1, M3), the gable (M2), the nave (M5–M6), and its roof (M19) were present, as expected. In more than 60% of the cases, plano-altimetric irregularities (M25) and the standing-out elements (M26) were observed. The vaults were present in different positions inside the church, such as in the nave,

the transept, etc., for about 42% of the cases; however, if consideration is limited to the more relevant elements, characterized by weight $\rho_k = 1$ (i.e., M8 and M9 according to Table 1), this proportion reduces to 31% of the cases. The other macroelements—the belltower (25%), transept (11%), dome (8%), and chapel (3%)—were registered with significantly lower frequency.

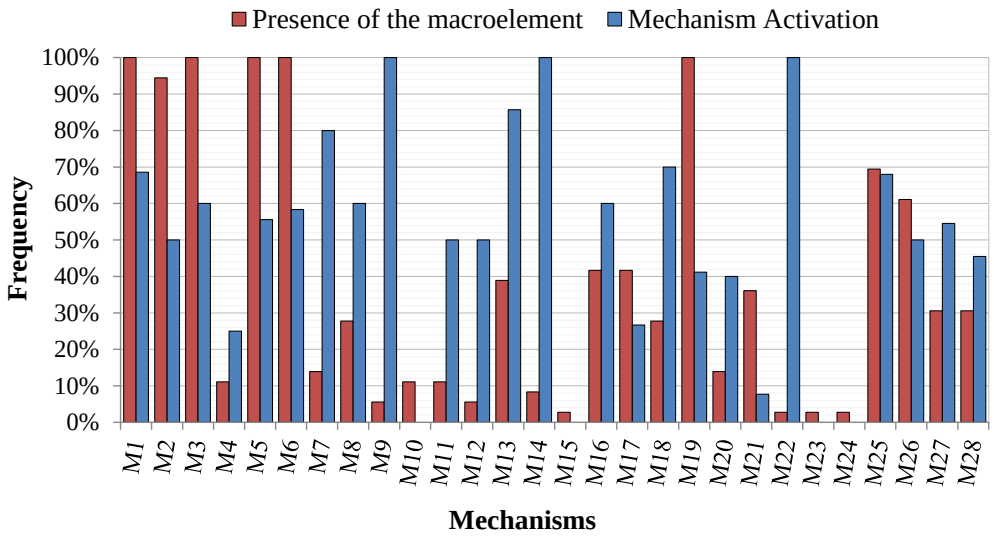

Figure 21. Presence and activation of the 28 mechanisms in the inspected churches.

Since the presence of the macroelement does not imply the mechanism activation, in distinct macroelements, the frequency of observed damages was calculated as the ratio of the number of churches showing the activation of the specific mechanism over the number of churches where the macroelements was present. For this purpose, it is important to underline that, in the case of destroyed churches, all mechanisms concerning the main macroelements (such as the façade, the nave, and the roof) were assumed to be activated. Similarly, if the collapse of a single macroelement was observed, all the related mechanisms were considered activated.

Concerning the activated mechanisms involving the façade (M1, M2, and M3), the following frequencies are detected:

- Overturning of the façade (M1)—it occurred in 24 churches, i.e., in 69% of cases in which the macroelement could be activated;
- Overturning of the gable (M2)—it was detected in the 50% of the possible cases;
- Shear mechanism in the façade (M3)—observed in the 60% of the reduced sample.

The fourth mechanism (M4) involves the porch or the narthex, architectural components found only in 11% of the inspected churches, which exhibited a negligible vulnerability level, since their activation percentage was 25%. As far as the nave is concerned, the mechanism should be distinguished between those affecting the vertical elements and those affecting the vaults. The first group includes the transversal vibration of the nave (M5) and the shear mechanism on the nave lateral walls (M6), mechanisms possible in all the surveyed churches, but triggered only in 56% and in 58% of the sample, respectively. Only 14% of the inspected religious buildings had a colonnade, but their longitudinal response (M7) was activated in 80% of the possible cases. The transept was present only in the 11% of the sample and its associated mechanisms cannot be regarded as representative, since the overturning (M10) was never triggered, and the shear failure (M11) was activated only in half of the possible cases. Only 39% of the inspected churches present triumphal arches, but the related mechanism (M13) was activated in 89% of the cases. Regarding the apses and presbytery walls, we can observe the following:

- The apse overturning (M16) could be developed in 15 churches, i.e., in 42% of the sample, and among them the activation frequency was the 60%;

- The shear failure of apse walls (M17) was triggered only in 27% of the possible cases.

The vaults, present in 42% of the sample, were mainly detected in the nave, the presbytery, and the apse. In detail, vaults of the central nave (M8) and in the presbytery and apse (M18) were observed in 10 churches (i.e., 28% of the sample). Concerning the vaults of the central nave (M8), the mechanism was triggered in 60% of the cases. Instead, more vulnerable were the vaults of the presbytery and the apse (M18), the mechanism of which was activated in 70% of the inspected buildings. Finally, the vaults of the aisles (M9) and of the transept (M12) are negligible since they characterize only 6% of the inspected churches. Nevertheless, in all cases the aisle vaults (M9) mechanism was activated, while the damage in the vaults of the transept (M12) occurred in only 50% of cases.

The dome and the lantern (M14) can be found only in three churches of the sample, but the related mechanism was always enabled. On the contrary, the collapse mechanism of the lantern (M15) was never triggered, but the related macroelement was observed in only one church. Among the most occurring mechanisms, hammering and damage in the roofs were very frequent, as follows:

- Damage on the nave roof (M19) could be verified in 94% of the sample, but it was activated only in 41% of the possible cases;
- The mechanisms in the transept roof (M20) were possible in only 14% of the churches and they had an occurrence probability of 40%;
- On the roof of the apse and the presbytery (M21), the mechanisms occurred in 36% of the religious buildings, and they took place only in 8% of the reduced sample.

The mechanisms related to the chapels (overturning, the shear failure of the walls, and the collapse of the vaults, i.e., M22, M23, and M24, respectively) seem to be extremely rare, since these components were present only in one inspected church; in this sample, only the overturning mechanism (M22) was triggered.

The interaction between elements characterized by different behaviors (M25) was verified in 69% of inspected buildings, and the related mechanism was effectively activated in 68% of the possible cases. Analogously, standing-out elements were observed in 61% of the sample, and their overturning (M26) developed in 50% of the cases.

Finally, belltowers were detected in 31% of the structures, and the related mechanisms—the global collapse (M27) and that of the bell cell (M28)—had trigger frequencies of 55% and 45%, respectively.

In summary, the most damaged architectural elements were the façade, the vaults, and the standing-out elements. Moreover, the damage caused by the interaction between elements, characterized by different behaviors, was frequent. Finally, even though domes were present in only three churches, in all these cases they were strongly damaged.

After identifying the activation of one of the mechanisms, the damage level reached was evaluated. Congruently to the approach adopted for assessing the mechanism activation, the maximum damage level was assumed for all collapsed macroelements and their related mechanisms. As an example, in the case of C10—St. Francis church—in which the façade collapsed (Figure 11), a damage level equal to 5 was assumed for all mechanisms concerning the façade (M1, M2, M3). In Figure 22, the mean damage level of each mechanism is represented by a scale from 1 to 5. The weight of the damage mechanisms is assessed according to the manual for the compilation of the survey In order to properly analyze the observed damaged mechanism, it is particularly interesting to relate the frequency of a given mechanism activation to the exposure of the related macroelement, i.e., the frequency of the presence of the macroelement in the surveyed churches.

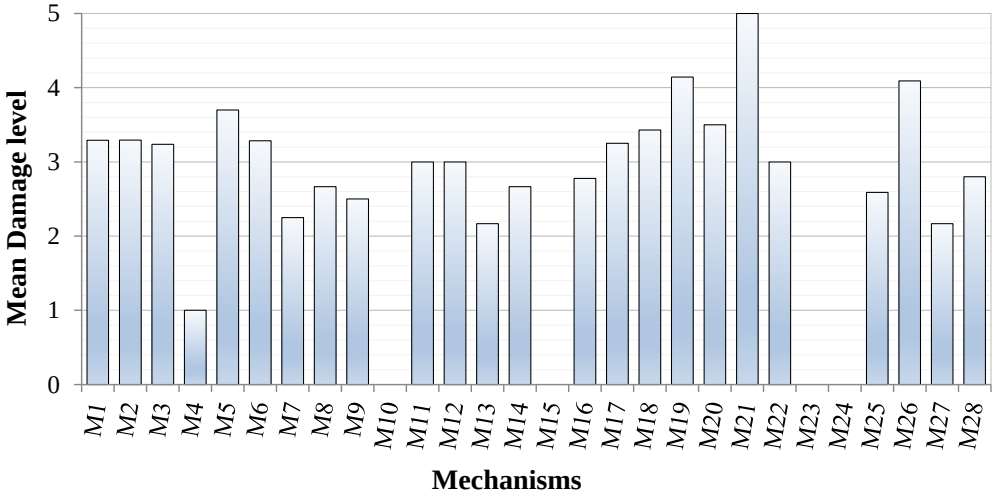

Figure 22. Mean damage levels of the mechanisms activated in the inspected churches.

It can be observed that the mechanisms M19 (nave roof), M21 (roof of apse and presbytery), and M26 (standing-out elements) are characterized by a higher mean damage level. However, damage of nave rooves, and the standing-out elements can be considered particularly serious because of their frequency of occurrence and, above all, because of their relevance in the churches' seismic performances. On the contrary, the apse was rarely present in the sample; therefore, the damage in its roof could not be considered meaningful. Among the mechanisms with an observed mean damage level higher than 3, the risk seems significant only for the façade (M1, M2, M3), the nave (M5 and M6), and the walls of the presbytery and the apse (M17). In fact, the vaults of the presbytery and the apse (M18), as well as the roof of the transept (M20), were infrequent in the sample, as previously indicated.

If macroelement is present in the church and the activation of the corresponding mechanism is observed, then it can be stated that the vaults of the presbytery and apse (M17) are slightly unsafe, and that the most critical mechanisms involve the façade and the related sidewalls (wall of the nave). In detail, concerning the elements composing the central nave, we can observe the following:

- The façade overturning (M1) simultaneously presents a 100% probability of occurrence, a probability of activation of 69%, and a mean damage level higher than 3. Specifically, through deeply analyzing the survey form, it can be detected that 44% of the sample is characterized by a damage level higher than 3 (serious damage). This percentage reduced to 28% if only those values higher than 4 (very serious damage) are considered.
- The gable overturning (M2) has a 94% probability of occurrence, and simultaneously, a 50% probability of activation and a mean damage level higher than 3. However, only 31% of the sample is characterized by a damage level higher than 3, and it should be considered that the façade collapsed in only 19% of cases.
- The shear mechanism of the façade (M3) was simultaneously characterized by a 100% probability of occurrence, a 60% probability of activation, and a mean damage level higher than 3. In detail, churches presenting a damage level higher than 3 comprise 42% of the sample, but when considering only very serious damages and collapses, this percentage reduces to 25%.
- The transversal vibration of the nave (M5) has a probability of occurrence of 100%, a probability of activation of 56%, and a mean damage level higher than 3. Additionally, in this case, 42% of the sample presents a damage level higher than 3, while the percentage decreases to 36% if accounting for only those values higher than 4.
- The shear mechanism in the nave sidewalls (M6) is characterized by a 100% probability of occurrence, 58% probability of activation, and a mean damage level higher than 3.

A proportion of 39% of the sample is characterized by damage levels higher than 3, while only 28% suffered the worst damages.

In conclusion, the overturning of the facade was the most dangerous mechanism we observed in the "Apennine church".

3.2. The Damage Index: Relationship with IMs and Usability Judgment

The above-described damage data were used to evaluate the average level of damage suffered by each church. According to [81], the index accounts for all possible kinematic mechanisms that can develop (the blue bars in Figure 21), regardless of their actual activation (red bars in Figure 21). Following the Italian post-seismic damage form, specifically designed for churches [57], the mean damage index can be evaluated as follows:

$$i_d = \frac{\sum_{k=1}^{28} d_k}{5n} \quad (2)$$

where d_k is the damage level of the k-th mechanism, defined by expert judgment, ranging from 0 (if any damage is observed) to 5 (in case of collapse); n is the number of the mechanisms that may be potentially activated when the related macroelement is present.

Alternatively, the Italian guidelines on the assessment and the mitigation of the seismic risk on cultural heritage [76] suggests estimating the damage index through a weighted sum of the damages occurred in all kinematics mechanisms, as follows:

$$i_{dW} = \frac{1}{5} \cdot \frac{\sum_{k=1}^{28} \rho_k \cdot d_k}{\sum_{k=1}^{28} \rho_k} \quad (3)$$

where ρ_k is the weight assigned to each activable mechanism according to the importance of the considered macroelement on the seismic performance of the church, according to the LV1 approach. For each mechanism, their possible values are the same as those reported in Table 1 [76].

For each inspected church, the following data are reported in Table 3: the seismic intensity of the measures suffered by the churches; the damage indexes, evaluated according to Equations (2) and (3); the usability judgment assigned to each church. Concerning the values of the damage indexes, it is interesting to note that Equations (2) and (3) led to very similar values for the considered sample, despite the application of specific weights in Equation (3) to account for the importance of some mechanisms. This result can be attributed to the peculiarities of the Apennine churches, composed mainly of basic macroelements associated with a unit weight according to the actual standards [76]. Instead, the weights assume a value of $\rho_k = 0.5$, only in the few cases of the less frequent macroelements. Undoubtedly, completely different values of i_{dW} could be presumed if the relative geometrical proportion of macroelements also is considered in the computation of the weighted observed damage index, as suggested in [77]. However, since the actual procedure of the post-seismic inspections disregards the measurement of the geometrical dimensions of the macroelements, a proper comparison between the damage index evaluated according to the actual Italian guidelines [76] and the one derived by the methodology proposed in [77] cannot be carried out.

Table 3. Church identification number (ID), peak ground accelerations (*PGA*), and macroseismic intensities (I_{MCS}), derived from ShakeMaps according to the geographical location of the church, the vulnerability index i_v, the observed and weighted observed damage index (i_d and i_{dW}, respectively), and the usability judgment.

ID	*PGA* (g)	I_{MCS}	i_d	i_{dW}	Usability Judgment
C1	0.04	5	0	0	Usable
C2	0.08	5	0	0	Usable

Table 3. *Cont.*

ID	*PGA* (g)	I_{MCS}	i_d	i_{dW}	Usability Judgment
C3	0.08	5	0.046	0.046	Usable
C4	0.04	5	0.10	0.09	Usable
C5	0.08	6	0.11	0.12	Usable
C6	0.04	5	0.22	0.21	Unusable
C7	0.04	5	0.43	0.43	Unusable
C8	0.76	6.5	0.38	0.38	Unusable
C9	0.08	6	0.60	0.60	Unusable
C10	0.72	10	0.88	0.88	Unusable
C11	0.768	10	0.82	0.86	Unusable
C12	0.768	10.5	1	1	Unusable
C13	0.08	5	0.03	0.03	Usable
C14	0.08	5	0.07	0.06	Usable after local interventions
C15	0.08	5	0.08	0.09	Partially Usable
C16	0.02	5	0.13	0.14	Partially Usable
C17	0.04	5	0.15	0.15	Usable after local interventions
C18	0.08	5	0.13	0.13	Unusable
C19	0.08	5	0.16	0.16	Usable
C20	0.08	5	0.18	0.17	Unusable
C21	0.48	6	0.2	0.16	Usable
C22	0.08	5	0.31	0.31	Unusable
C23	0.08	5	0.30	0.30	Unusable
C24	0.12	5	0.35	0.34	Unusable
C25	0.48	7	0.78	0.78	Unusable
C26	0.56	10.5	1	1	Unusable
C27	0.44	9.5	1	1	Unusable
C28	0.44	9.5	1	1	Unusable
C29	0.52	10.5	1	1	Unusable
C30	0.08	5	0.20	0.21	Partially Usable
C31	0.04	5	0.28	0.27	Unusable
C32	0.08	5	0.25	0.26	Unusable
C33	0.08	5	0.20	0.21	Unusable
C34	0.08	5	0.27	0.27	Unusable
C35	0.48	6	0.62	0.62	Unusable
C36	0.08	6	0.51	0.51	Unusable

Due to the similarity of the global and weighted damage indexes for the considered sample, only the global damage index, i_d (Equation (2)), is considered in the following. Concerning the obtained results, it could be concluded that:

- 25% of the inspected churches were severely damaged or collapsed;
- 17% of the dataset experienced extended damage and consequently observed damage indexes ranging from 0.3 to 0.6;
- 58% of the inspected churches were characterized by limited damage (i.e., observed damage index from 0 to 0.3).

To evaluate a relationship between the damage index and the maximum intensity measures suffered by the churches, the damage index, i_d, was represented versus two seismic intensity measures: the observed Mercalli–Cancani–Sieberg macroseismic intensities, I_{MCS}, and the *PGA*. The I_{MCS}, deduced from [82], is defined according to an empirical qualitative scale representative of the effects of an earthquake on people, objects, buildings, and environment, evaluated by observing the percentage of buildings damaged or destroyed and the behavior of people. Therefore, it is not a measure in the strict sense, and it could not characterize the effective severity of an earthquake in less urbanized areas, such as those in which many of the surveyed churches are placed. The *PGA*, instead, is the actual measurement of the maximum acceleration exerted by an earthquake on the ground, and it is punctually recorded by means of the accelerometers belonging to the finalized Italian Strong Motion Network. A synthetic representation of the *PGA* suffered by a region after an earthquake is depicted by the ShakeMaps [83], developed by the Italian National Institute of Geophysics and Volcanology, according to proper attenuation laws; this is particularly accurate in sites where the geognostic and geophysical investigations are available.

Analyzing the relationship between i_d and the macroseismic intensity (Figure 23a), it can be observed that, for lower intensities (I_{MCS} = V), the distribution of the observed damage index spreads between 0 and 0.43; meanwhile, higher values (I_{MCS} > VII), cataloged as ruinous–destructive for ordinary buildings, according to the I_{MCS} scale, were suffered by churches whose damage index is above 0.8, except for one case, with i_d equal to 0.78. Concerning I_{MCS} values equal to VI, the damage index is very scattered. Since there is not a direct correlation between the observed I_{MCS} and the *PGA*, some overlapping can be observed in Figure 23b. Noteworthy aspects related to the inspected churches and seismic intensity measures are the following:

- The locations of most of the inspected churches are characterized by the V degree of the I_{MCS} scale, corresponding to *PGA* values between 0.02 g and 0.08 g (except for one struck by a *PGA* of 0.12 g).
- Even if the VI degree of the I_{MCS} corresponds to a wide range of *PGA* (from 0.08 g to 0.48 g), only 5 churches of the inspected sample are in such an area.
- The degrees of I_{MCS} greater than VI are associated with high *PGA* values, ranging between 0.44 g and 0.76 g.

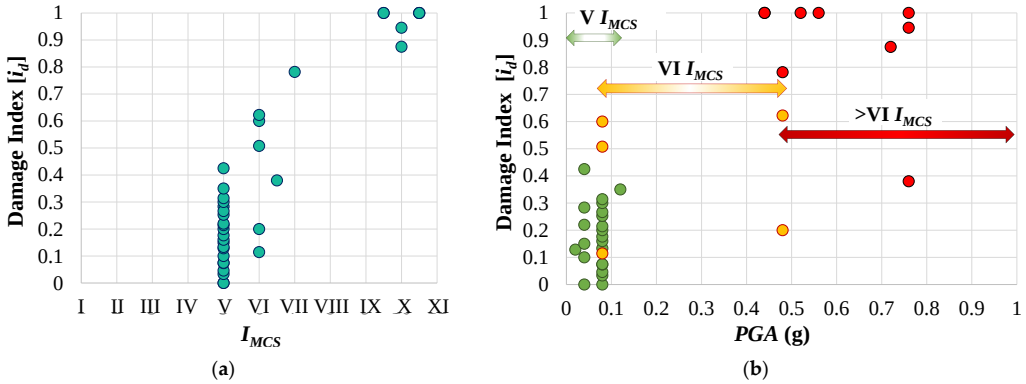

Figure 23. Damages directly observed by the authors in the churches sample compared to: (**a**) *PGA* (g); (**b**) macroseismic intensity, I_{MCS}.

Concerning the usability assessment, the church form considers six possible categories, selected among the following: usable; partially usable, i.e., only a portion of the structure can be used safely; usable after local interventions; temporarily unusable, i.e., requiring a more detailed investigation; unusable; unusable due to external hazard. In Figure 24, the usability judgment is represented with respect to the observed *PGA* (Figure 24a), the global damage index (Figure 24b), and the vulnerability index (Figure 24c). For the following analysis, the "Usable after local intervention" outcome, consisting of only two churches,

was added to the "Partially usable" group, composed of three churches. Analyzing the usability outcomes presented in Figure 24a and Table 2, the following should be noted:

- Only 8 (22.2%) churches of the sample are usable, 5 (13.9%) are partially usable, and 23 (63.9%) are unusable.
- All usable and partially usable churches suffered a *PGA* value lower than 0.08 g, with the limited exception of one church (C21), for which the assigned *PGA* was equal to 0.48 g. It is worth noting that this church is in a small village, in which the masonry buildings experienced minor seismic damages in the surrounding areas.
- Unusable churches suffered a *PGA* ranging from 0.04 to 0.77 g; in detail, 10 churches were characterized by *PGA* > 0.40 g, whilst 13 churches were struck by *PGA* ranging between 0.04 and 0.12 g.
- Overall, all churches with a *PGA* > 0.08 g were unusable and seriously damaged, with the only exception of 1 usable building.
- It is difficult to identify a proper correlation between the intensity measure and the usability judgment for low values of *PGA*. In fact, church vulnerability plays a key role in the judgment of damages and usability.

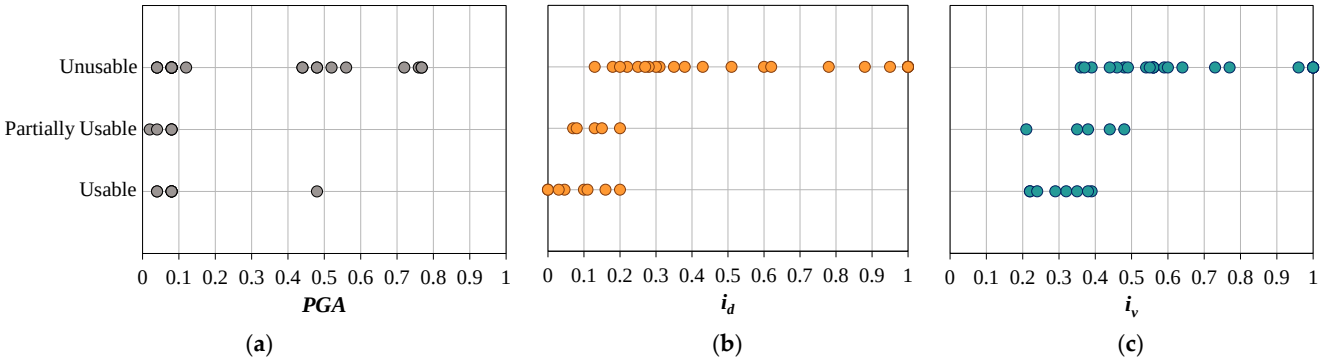

Figure 24. Correlation between usability assessment, *PGA* (**a**), global damage index evaluated according to Equation (2) (**b**), and vulnerability index defined according to LV1 approach (**c**).

Analyzing the usability outcomes in relation to the damage index (Figure 24b and Table 3), the following should be noted:

- The damage index varies from 0 to 1, with a mean value equal to 0.081 and 0.550 for usable and unusable churches, respectively; all churches with a damage index greater than 0.2 are unusable.
- Usable and partially usable churches are characterized by damage index varying between 0 and 0.2.
- Unusable churches can be subdivided in two families: 20 churches characterized by i_d > 0.2, and 3 churches (C18, C20, C33) with lower values. The latter suffered the 2009 L'Aquila earthquake, and the previous damages were eventually unrepaired (C18 and C33). Therefore, such moderately vulnerable churches (i_v falls in the range of 0.36–0.46) had their preexisting crack pattern enlarged after the seismic sequence in 2016, even in the face of a PGA equal to 0.08 g. However, it is worth underlining that the low i_d obtained in the above cases is due to highly localized damages (C18) or to the significant number of macroelements present in the structures compared with the activated mechanism (C20, C33).

Finally, concerning the usability outcomes in relation to the vulnerability index (Figure 24c, Tables 2 and 3), the following can be observed:

- Usable churches had a maximum vulnerability index equal to 0.39, with an average value of 0.30.
- The 5 partially usable churches are characterized by i_v in the range 0.21–0.48, with an average value of 0.37.

- For values greater than 0.5, all churches are unusable; however, there are 7 unusable churches characterized by i_v greater than 0.36.
- Unusable churches presented an average vulnerability index of 0.56.

According to the obtained results (Figure 24b), the usability judgment shows a low correlation with the mean damage index. Conversely, it has become well established that i_d does not frequently depict the actual scale of the suffered damages and the usability assessment of ancient masonry churches [77,84], the seismic behavior of which is not characterized by the activation (progressive or simultaneous) of all local mechanisms. When only one macroelement collapses, or a very limited number of kinematic mechanisms are triggered, one finds that the church is declared unusable, and the observed damage index, i_d, results are exceptionally low. This is, for example, the case of C23 (Holy Mary Abbey in Montesanto) (Figure 25), where the roof was completely collapsed: the church was clearly unusable, but the observed damage index is equal to 0.35. Similarly, the churches characterized by a preexisting crack pattern as a consequence of the 2009 L'Aquila Earthquake—in the case of the structures located in the Abruzzo region—or due to the consecutive earthquakes of the 2016/2017 seismic sequence, show worsening conditions affecting the already damaged macroelements. In this situation, the church is declared unusable due to the overall observed damage pattern—the result of several shakes occurring over a long time—even when the mean damage index, i_d, is low, and when the seismic accelerations of the main earthquake occurring before the inspection were small.

(**a**) (**b**)

Figure 25. Limited damages and loss of usability in the Abbey in Montesanto (C25): (**a**) absence of damage in the façade and roof collapse; (**b**) absence of damage in the lateral wall.

As a matter of fact, the mean damage index is not a reliable representation of the actual earthquake damage to a church since it is evaluated in the hypothesis of contemporary activation of all possible mechanisms. Therefore, generally, small values could characterize the mean damage index, i_d, defined according to the guidelines in force, even in the presence of severe but localized damages; moreover, such low values do not reflect the usability judgment.

Among the critical issues in the definition of the mean damage index, i_d, two factors which are disregarded seem to be crucial—the peaks of the damage and the effects of the directionality of the seismic action. To overcome such a criticism, Lagomarsino et al. [77] introduced new additional damage scores: two considering the directionality of the response (differentiated for the two main directions of the church) and one to evaluate the presence of peaks of damage. However, it is worth noting that Lagomarsino et al. [77] introduced a new form that could account for 150 potential mechanisms, to be as general and flexible as possible. Moreover, the weights evaluated from the macroelement geometrical size are suggested rather than fixed, based on the element's importance in the structural context.

Unfortunately, due to the absence of certain data, such updates make the application of the approach proposed in [77] impossible, since only the content of the actual damage surveys [57] is available.

4. Conclusions

This work presents the results of the survey inspections carried out after the 2016 Central Italy seismic sequence on 36 historical masonry churches, with the aim of identifying the structural damages and assessing their eventual usability. The analyzed monuments were located between 5 and 50 km from the epicenter, and most of them presented similar architectural features depicting the typical "Apennine church": a single nave, a simple facade with a rose window over the entrance, a triangular/rectangular gable, a double pitched timber roof, and a belltower beside the church. The typical masonry walls consist of a double layer of local irregular stones and poor-quality mortar. The post-seismic damage assessment provided data about the architectural morphology, the most frequently observed damage mechanisms, and the usability judgment for each church. These data were carefully analyzed, and they were employed to evaluate the seismic vulnerability of each church, defined according to the simplified LV1 procedure, proposed by the Italian guidelines.

Concerning the results obtained for the vulnerability indexes, a predominant low–medium vulnerability was observed for the considered sample ($i_v \leq 0.6$). This could explain the absence of a proper correlation between the usability index and the seismic intensities for low values of PGA. In such cases, the church vulnerability plays a key role in the damages and, therefore, influences the judgment of the usability. On the other hand, the authors' inspections outline that, for 11 cases out of 18, the unusable churches were characterized by a vulnerability index higher than 0.50; considering the entire sample of the unusable churches, the estimated average value of the vulnerability index was 0.56.

Regarding the post-earthquake damage observation, the churches declared unusable usually presented a damage level greater than 3 in at least one macroelement. Moreover, the high vulnerability of the façade was observed. The out-of-plane mechanism of the façade occurred in 69% of cases, causing serious damages in 44% of the sample. The shear mechanism of the façade showed a similar percentage (42% of the sample was characterized by a damage level higher than 3), but it occurred less frequently, i.e., in 60% of cases.

Even if the number of presented churches is low, the analysis of the sample made it possible to highlight some critical issues of the actual definition of the damage index, the global damage index, i_d, and its poor correlation with the final usability judgment.

According to the Italian guidelines on the assessment and the mitigation of the seismic risk of the cultural heritage, the damage index, i_d, accounts for all mechanisms which could develop in a church. Therefore, concentrated damages have a low impact on the i_d value, which is often not representative of the effective damage state, as has been observed by other authors. In the considered sample, the usable churches present a mean value of 0.081, while all churches with a damage index greater than 0.2 were declared unusable. Moreover, i_d shows a low association with usability assessment.

Of course, since the main outlined findings are related to a small sample of 36 churches, the observed outcomes should be confirmed by using a more extensive database of churches located in the region struck by the 2016 Central Italy earthquake.

Author Contributions: Conceptualization, S.C., S.I. and B.F.; methodology, M.Z., S.I. and B.F.; validation, S.I. and B.F.; investigation, S.C., B.F, S.I. and M.Z.; resources, M.Z.; data curation, S.I., S.C., and B.F; writing—original draft preparation, M.Z. and S.I.; writing—review and editing, M.Z., S.I., S.C. and B.F.; visualization, B.F.; project administration, B.F. All authors have read and agreed to the published version of the manuscript.

Funding: This work was developed under the financial support of the Italian Civil Protection Department within the DPC-ReLUIS 2019–2021 research project, which is gratefully acknowledged.

Institutional Review Board Statement: Not applicable.

Informed Consent Statement: Not applicable.

Data Availability Statement: The raw/processed data required to reproduce these findings cannotbe shared at this time as the data also forms part of an ongoing study.

Acknowledgments: The Italian Civil Protection Department, the Italian Ministry of Cultural Heritage (MiBACT), and ReLUIS Consortium are gratefully acknowledged for involving the authors in the usability inspections of monuments.

Conflicts of Interest: The authors declare no conflict of interest.

References

1. Branno, A.; Esposito, E.; Luongo, G.; Marturano, A.; Porfido, S.; Rinaldis, V. The largest earthquakes of the Apennines, southern Italy. In Proceedings of the International Symposiym of Engineering Geology Problems in Seismic Areas, Bari, Italy, 13–19 April 1986; Volume 4, pp. 3–14.
2. Borre, K.; Cacon, S.; Cello, G.; Kontny, B.; Kostak, B.; Likke Andersen, H.; Moratti, G.; Piccardi, L.; Stemberk, J.; Tondi, E.; et al. The COST project in Italy: Analysis and monitoring of seismogenic faults in the Gargano and Norcia areas (central-southern Apennines, Italy). *J. Geodyn.* **2003**, *36*, 3–18. [CrossRef]
3. Galli, P. Recurrence times of central-southern Apennine faults (Italy): Hints from palaeoseismology. *Terra Nova* **2020**, *32*, 399–407. [CrossRef]
4. Rovida, A.; Locati, M.; Camassi, R.; Lolli, B.; Gasperini, P. The Italian earthquake catalogue CPTI15. *Bull. Earthq. Eng.* **2020**, *18*, 2953–2984. [CrossRef]
5. Proietti, G. Soprintendenza Generale per gli Interventi Post-Sismici in Campania e Basilicata. In *Dopo la Polvere: Rilevazione Degli Interventi di Recupero Post-Sismico del Patrimonio Archeologico, Architettonico ed Artistico delle Regioni Campania e Basilicata Danneggiato dal Terremoto del 23 Novembre 1980 e del 14 Febbraio 1981*; Istituto Poligrafico e Zecca dello Stato: Roma, Italy, 1994; Volume 5.
6. Mazzoleni, D.; Sepe, M. *Rischio Sismico, Paesaggio, Architettura: L'Irpinia, Contributi per un Progetto*; CRdC-AMRA: Naples, Italy, 2005. (In Italian)
7. D'Ayala, D.F.; Paganoni, S. Assessment and analysis of damage in L'Aquila historic city centre after 6th April 2009. *Bull. Earthq. Eng.* **2011**, *9*, 81–104. [CrossRef]
8. Drago, C.; Ferlito, R.; Zucconi, M. Equivalent damage validation by variable cluster analysis. In *AIP Conference Proceedings*; AIP Publishing LLC: Melville, NY, USA, 2016; Volume 1738, p. 270014.
9. Zucconi, M.; Sorrentino, L.; Ferlito, R. Principal component analysis for a seismic usability model of unreinforced masonry buildings. *Soil Dyn. Earthq. Eng.* **2017**, *96*, 64–75. [CrossRef]
10. Zucconi, M.; Sorrentino, L.; Ferlito, R. Verification of a usability model for unreinforced masonry buildings with data from the 2002 Molise, southern Italy, eartqhuake. In Proceedings of the 10th International Masonry Conference, IMC 2018, Milan, Italy, 9–11 July 2018; pp. 680–688.
11. Zucconi, M.; Ferlito, R.; Sorrentino, L. Validation and extension of a statistical usability model for unreinforced masonry buildings with different ground motion intensity measures. *Bull. Earthq. Eng.* **2020**, *18*, 767–795. [CrossRef]
12. Zucconi, M.; Sorrentino, L. Census-Based Typological Damage Fragility Curves and Seismic Risk Scenarios for Unreinforced Masonry Buildings. *Geosciences* **2022**, *12*, 45. [CrossRef]
13. Bruneau, M. State-of-the-art report on seismic performance of unreinforced masonry buildings. *J. Struct. Eng.* **1994**, *120*, 230–251. [CrossRef]
14. Decanini, L.; De Sortis, A.; Goretti, A.; Langenbach, R.; Mollaioli, F.; Rasulo, A. Performance of masonry buildings during the 2002 Molise, Italy, earthquake. *Earthq. Spectra* **2004**, *20*, S191–S220. [CrossRef]
15. Penna, A.; Morandi, P.; Rota, M.; Manzini, C.F.; Da Porto, F.; Magenes, G. Performance of masonry buildings during the Emilia 2012 earthquake. *Bull. Earthq. Eng.* **2014**, *12*, 2255–2273. [CrossRef]
16. Coccia, S.; Di Carlo, F.; Imperatore, S. Strength reduction factor for out-of-plane failure mechanisms of masonry walls. In *Brick and Block Masonry: Trends, Innovations and Challenges—Proceedings of the 16th International Brick and Block Masonry Conference, IBMAC 2016, Padova, Italy, 26–30 June 2016*; CRC Press: Boca Raton, FL, USA, 26–30 June; pp. 137–144.
17. Zucconi, M.; Ferlito, R.; Sorrentino, L. Typological Damage Fragility Curves for Unreinforced Masonry Buildings affected by the 2009 L'Aquila, Italy Earthquake. *Open Civ. Eng. J.* **2021**, *15*, 117–134. [CrossRef]
18. Ministero per i Beni Culturali e Ambientali, Bollettino d'arte. *Sisma del 1980: Effetti sul Patrimonio Artistico della Campania e Basilicata-Campania*; Supplemento n.2; Istituto Poligrafico E Zecca dello Stato: Roma, Italy, 1982. (In Italian)
19. Cifani, G.; Lemme, A.; Podestà, S. *Beni Monumentali e Terremoto. Dall'emergenza alla Ricostruzione*; DEI-Tipografia del Genio Civile: Roma, Italy, 2005. (In Italian)
20. Binda, L.; Saisi, A. Research on historic structures in seismic areas in Italy. *Prog. Struct. Eng. Mater.* **2005**, *7*, 71–85. [CrossRef]
21. da Porto, F.; Silva, B.; Costa, C.; Modena, C. Macro-scale analysis of damage to churches after earthquake in Abruzzo (Italy) on April 6, 2009. *J. Earthq. Eng.* **2012**, *16*, 739–758. [CrossRef]

22. Colonna, S.; Imperatore, S.; Zucconi, M.; Ferracuti, B. Post-seismic damage assessment of a historical masonry building: The case study of a school in Teramo. In Proceedings of the International Conference on Mechanics of Masonry Structures Strengthened with Composites Materials, MuRiCo5, Bologna, Italy, 28–30 June 2017; pp. 620–627.
23. De Matteis, G.; Brando, G.; Corlito, V.; Criber, E.; Guadagnuolo, M. Seismic vulnerability assessment of churches at regional scale after the 2009 L'Aquila earthquake. *Int. J. Mason. Res. Innov.* **2019**, *4*, 174–196. [CrossRef]
24. Colonna, S.; Imperatore, S.; Ferracuti, B. Fragility curves of masonry churches façades. In Proceedings of the 7th International Conference on Computational Methods in Structural Dynamics and Earthquake Engineering, COMPDYN 2019, Crete, Greece, 24–26 June 2019; Volume 1, pp. 718–731.
25. Gaudiosi, G.; Alessio, G.; Nappi, R.; Noviello, V.; Spiga, E.; Porfido, S. Evaluation of Damages to the Architectural Heritage of Naples as a Result of the Strongest Earthquakes of the Southern Apennines. *Appl. Sci.* **2020**, *10*, 6880. [CrossRef]
26. Nardone, L.; Gizzi, F.T.; Maresca, R. Ground Response and Historical Buildings in Avellino (Campania, Southern Italy): Clues from a Retrospective View Concerning the 1980 Irpinia-Basilicata Earthquake. *Geosciences* **2020**, *10*, 503. [CrossRef]
27. Benenato, A.; Lignola, G.P.; Imperatore, S.; Ferracuti, B. Probabilistic seismic fragility for rocking masonry façades using cloud analysis. In Proceedings of the 8th International Conference on Computational Methods in Structural Dynamics and Earthquake Engineering, Compdyn 2021, Athens, Greece, 28–30 June 2021; Volume 2021.
28. Reluis-Consorzio della Rete dei Laboratori Universitari di Ingegneria Sismica e Strutturale. Available online: http://www.reluis.it/images/stories/Le_attività_del_DPC_durante_e_dopo_Aquila_2009_Dolce.pdf (accessed on 5 November 2020).
29. Dipartimento della Protezione Civile–Presidenza del Consiglio dei Ministri. Available online: http://www.protezionecivile.gov.it/jcms/it/terremoto_centro_italia_2016 (accessed on 5 November 2020).
30. Giuffrè, A. *Letture Sulla Meccanica Delle Murature Storiche*; Edizioni Kappa: Roma, Italy, 1991; pp. 1–52.
31. Giuffrè, A. *Sicurezza e Conservazione del Centri Storici: Il Caso Ortigia*; Editori Laterza: Bari, Italy, 1993; pp. 1–123.
32. Como, M. Equilibrium and collapse analysis of masonry bodies. In *Masonry Construction*; Springer: Dordrecht, The Netherlands, 1992; pp. 185–194.
33. Doglioni, F.; Moretti, A.; Petrini, V.; Angeletti, P. Le chiese e il terremoto. Dalla vulnerabilità constatata nel terremoto del Friuli al miglioramento antisismico nel restauro. In *Verso Una Politica di Prevenzione*; Edizioni Lint: Trieste, Italy, 1994; pp. 108–204.
34. Lagomarsino, S.; Podesta, S. Damage and vulnerability assessment of churches after the 2002 Molise, Italy, earthquake. *Earthq. Spectra* **2004**, *20*, S271–S283. [CrossRef]
35. Lagomarsino, S.; Podesta, S. Seismic vulnerability of ancient churches: I. Damage assessment and emergency planning. *Earthq. Spectra* **2004**, *20*, 377–394. [CrossRef]
36. Lagomarsino, S.; Podesta, S. Seismic vulnerability of ancient churches: II. Statistical analysis of surveyed data and methods for risk analysis. *Earthq. Spectra* **2004**, *20*, 395–412. [CrossRef]
37. Valente, M.; Milani, G. Damage survey, simplified assessment, and advanced seismic analyses of two masonry churches after the 2012 Emilia earthquake. *Int. J. Archit. Herit.* **2018**, *13*, 901–924. [CrossRef]
38. Borri, A.; Corradi, M.; Castori, G.; Sisti, R.; De Maria, A. Analysis of the collapse mechanisms of medieval churches struck by the 2016 Umbrian earthquake. *Int. J. Archit. Herit.* **2018**, *13*, 215–218. [CrossRef]
39. Dizhur, D.; Ingham, J.; Moon, L.; Griffith, M.; Schultz, A.; Senaldi, I.; Magenes, G.; Dickie, J.; Lissel, S.; Centeno, J.; et al. Performance of masonry buildings and churches in the 22 February 2011 Christchurch earthquake. *Bull. N. Zeal. Soc. Earthq. Eng.* **2011**, *44*, 279–296. [CrossRef]
40. Lagomarsino, S. Damage assessment of churches after L'Aquila earthquake (2009). *Bull. Earthq. Eng.* **2012**, *10*, 73–92. [CrossRef]
41. Leite, J.; Lourenco, P.B.; Ingham, J.M. Statistical Assessment of Damage to Churches Affected by the 2010–2011 Canterbury (New Zealand) Earthquake Sequence. *J. Earthq. Eng.* **2013**, *17*, 73–97. [CrossRef]
42. Sorrentino, L.; Liberatore, L.; Decanini, L.D.; Liberatore, D. The performance of churches in the 2012 Emilia earthquakes. *Bull. Earthq. Eng.* **2014**, *12*, 2299–2331. [CrossRef]
43. De Matteis, G.; Criber, E.; Brando, G. Damage probability matrices for three-nave masonry churches in Abruzzi after the 2009 L'Aquila earthquake. *Int. J. Archit. Herit.* **2016**, *10*, 120–145.
44. Colonna, S.; Imperatore, S.; Ferracuti, B. The 2016 central Italy earthquake: Damage and vulnerability assessment of churches. Proceedings of 10th International Masonry Conference, IMC 2018; Milan, Italy, 9–11 July 2018; Milani, G., Taliercio, A., Garrity, S., Eds.; International Masonry Society: Whyteleafe, UK, 2018; pp. 2425–2440.
45. Fuentes, D.D.; Baquedano Julià, P.A.; D'Amato, M.; Laterza, M. Preliminary seismic damage assessment of Mexican churches after September 2017 earthquakes. *Int. J. Archit. Herit.* **2019**, *15*, 505–525. [CrossRef]
46. Palazzi, N.C.; Rovero, L.; De La Llera, J.C.; Sandoval, C. Preliminary assessment on seismic vulnerability of masonry churches in central Chile. *Int. J. Archit. Herit.* **2019**, *14*, 829–848. [CrossRef]
47. Palazzi, N.C.; Favier, P.; Rovero, L.; Sandoval, C.; de la Llera, J.C. Seismic damage and fragility assessment of ancient masonry churches located in central Chile. *Bull. Earthq. Eng.* **2020**, *18*, 3433–3457. [CrossRef]
48. Salzano, P.; Casapulla, C.; Ceroni, F.; Prota, A. Seismic vulnerability and simplified safety assessments of masonry churches in the Ischia Island (Italy) after the 2017 earthquake. *Int. J. Archit. Herit.* **2020**, *16*, 136–162. [CrossRef]
49. Galli, P.; Peronace, E.; Bramerini, F.; Castenetto, S.; Naso, G.; Cassone, F.; Pallone, F. The MCS intensity distribution of the devastating 24 August 2016 earthquake in central Italy (M_W 6.2). *Ann. Geophys.* **2016**, *59*. [CrossRef]

50. Pischiutta, M.; Akinci, A.; Malagnini, L.; Herrero, A. Characteristics of the strong ground motion from the 24th August 2016 Amatrice earthquake. *Ann. Geophys.* **2016**, *59*. [CrossRef]
51. INGVterremoti. Available online: https://ingvterremoti.com/2017/04/28/sequenza-in-italia-centrale-aggiornamento-del-28-aprile/ (accessed on 29 December 2021).
52. Pucci, S.; De Martini, P.M.; Civico, R.; Villani, F.; Nappi, R.; Ricci, T.; Azzaro, R.; Brunori, C.A.; Ciacagli, M.; Cinti, F.R.; et al. Coseismic ruptures of the 24 August 2016, Mw 6.0 Amatrice earthquake (central Italy). *Geophys. Res. Lett.* **2017**, *44*, 2138–2147. [CrossRef]
53. Civico, R.; Pucci, S.; Villani, F.; Pizzimenti, L.; De Martini, P.M.; Nappi, R.; Open EMERGEO Working Group. Surface ruptures following the 30 October 2016 M w 6.5 Norcia earthquake, central Italy. *J. Maps* **2018**, *14*, 151–160. [CrossRef]
54. Luiso, P.; Paoletti, V.; Nappi, R.; Gaudiosi, G.; Cella, F.; Fedi, M. Testing the value of a multi-scale gravimetric analysis in characterizing active fault 2 geometry at hypocentral depths: The 2016–2017 Central Italy seismic sequence. *Ann. Geophys.* **2018**, *61*. [CrossRef]
55. Villani, F.; Civico, R.; Pucci, S.; Pizzimenti, L.; Nappi, R.; De Martini, P.M. A database of the coseismic effects following the 30 October 2016 Norcia earthquake in Central Italy. *Sci. Data* **2018**, *5*, 180049. [CrossRef]
56. Di Ludovico, M.; De Martino, G.; Santoro, A.; Prota, A.; Manfredi, G.; Calderini, C.; Carocci, C.; Da Porto, F.; Dall'Asta, A.; De Santis, S.; et al. Usability and damage assessment of public buildings and churches after the 2016 Central Italy earthquake. In Proceedings of the 7th International Conference Earthquake Geotechnical Engineering for Protection and Development of Environment and Constructions, Rome, Italy, 17–20 June 2019.
57. MiBAC. Form A-DC PCM-DPC. Scheda per il Rilievo del Danno ai Beni Culturali—Chiese. 2006. Available online: https://www.beniculturali.it/mibac/multimedia/MiBAC/documents/1338454237471_allegato4.pdf (accessed on 5 March 2021).
58. MiBAC. Form B-DP PCM-DPC. Scheda per il Rilievo Del Danno ai Beni Culturali—Palazzi. 2006. Available online: https://www.beniculturali.it/mibac/multimedia/MiBAC/documents/1338454343145_allegato3.pdf (accessed on 5 March 2021).
59. MiBACT. *Direttiva 23 Aprile 2015: Aggiornamento Della Direttiva 12 Dicembre 2013, Relativa alle "Procedure per la Gestione Delle Attività di Messa in Sicurezza e Salvaguardia del Patrimonio Culturale in Caso di Emergenze Derivanti da Calamità Naturali"*; G.U. No. 169, 23/07/2015; Libreria dello Stato: Rome, Italy, 2015. (In Italian)
60. Penna, A.; Calderini, C.; Sorrentino, L.; Carocci, C.F.; Cescatti, E.; Sisti, R.; Borri, A.; Modena, C.; Prota, A. Damage to churches in the 2016 central Italy earthquakes. *Bull. Earthq. Eng.* **2019**, *17*, 5763–5790. [CrossRef]
61. Sferrazza Papa, G.; Silva, B. Assessment of post-earthquake damage: St. Salvatore church in Acquapagana, central Italy. *Buildings* **2018**, *8*, 45. [CrossRef]
62. Sorrentino, L.; Doria, M.; Tassi, V.; Liotta, M.A. Performance of a Far-Field Historical Church during the 2016–2017 Central Italy Earthquakes. *J. Perform. Constr. Facil.* **2019**, *33*, 04019016. [CrossRef]
63. Grazzini, A.; Chiabrando, F.; Foti, S.; Sammartano, G.; Spanò, A. A multidisciplinary study on the seismic vulnerability of St. Agostino church in Amatrice following the 2016 seismic sequence. *Int. J. Archit. Herit.* **2020**, *14*, 885–902. [CrossRef]
64. Giordano, E.; Clementi, F.; Nespeca, A.; Lenci, S. Damage assessment by numerical modeling of sant'agostino's sanctuary in offida during the central italy 2016–2017 Seismic Sequence. *Front. Built Environ.* **2019**, *4*, 87. [CrossRef]
65. Jain, A.; Acito, M.; Chesi, C. Seismic sequence of 2016–17: Linear and non-linear interpretation models for evolution of damage in San Francesco church, Amatrice. *Eng. Struct.* **2020**, *211*, 110418. [CrossRef]
66. Papa, G.S.; Tateo, V.; Parisi, M.A.; Casolo, S. Seismic response of a masonry church in Central Italy: The role of interventions on the roof. *Bull. Earthq. Eng.* **2021**, *19*, 1151–1179. [CrossRef]
67. Clementi, F.; Ferrante, A.; Giordano, E.; Dubois, F.; Lenci, S. Damage assessment of ancient masonry churches stroked by the Central Italy earthquakes of 2016 by the non-smooth contact dynamics method. *Bull. Earthq. Eng.* **2020**, *18*, 455–486. [CrossRef]
68. Clementi, F. Failure Analysis of Apennine Masonry Churches Severely Damaged during the 2016 Central Italy Seismic Sequence. *Buildings* **2021**, *11*, 58. [CrossRef]
69. Ferrante, A.; Giordano, E.; Clementi, F.; Milani, G. FE vs. DE Modeling for the Nonlinear Dynamics of a Historic Church in Central Italy. *Geosciences* **2021**, *11*, 189. [CrossRef]
70. Hofer, L.; Zampieri, P.; Zanini, M.A.; Faleschini, F.; Pellegrino, C. Seismic damage survey and empirical fragility curves for churches after the August 24, 2016 Central Italy earthquake. *Soil Dyn. Earthq. Eng.* **2018**, *111*, 98–109. [CrossRef]
71. De Matteis, G.; Zizi, M. Preliminary analysis on the effects of 2016 Central Italy earthquake on one-nave churches. In *Structural Analysis of Historical Constructions*; Aguilar, R., Torrealva, D., Moreira, S., Pando, M.A., Ramos, L.F., Eds.; RILEM Bookseries; Springer: Cham, Switzerland, 2019; Volume 18, pp. 1268–1279.
72. De Matteis, G.; Zizi, M. Seismic damage prediction of masonry churches by a PGA-based approach. *Int. J. Archit. Herit.* **2019**, *13*, 1165–1179. [CrossRef]
73. Canuti, C.; Carbonari, S.; Dall'Asta, A.; Dezi, L.; Gara, F.; Leoni, G.; Morici, M.; Petrucci, E.; Zona, A. Post-earthquake damage and vulnerability assessment of churches in the Marche Region struck by the 2016 Central Italy seismic sequence. *Int. J. Archit. Herit.* **2019**, *15*, 1000–1021. [CrossRef]
74. Cescatti, E.; Salzano, P.; Casapulla, C.; Ceroni, F.; da Porto, F.; Prota, A. Damages to masonry churches after 2016–2017 Central Italy seismic sequence and definition of fragility curves. *Bull. Earthq. Eng.* **2019**, *18*, 297–329. [CrossRef]
75. Morici, M.; Canuti, C.; Dall'Asta, A.; Leoni, G. Empirical predictive model for seismic damage of historical churches. *Bull. Earthq. Eng.* **2020**, *18*, 6015–6037. [CrossRef]

76. Direttiva del Presidente Consiglio dei Ministri (DPCM) del 9 Febbraio 2011. *Valutazione e Riduzione del Rischio Sismico del Patrimonio Culturale con Riferimento alle Norme Tecniche per le Costruzioni di cui al DM 14 Gennaio 2008*; GU Serie Generale No. 47, 26-02-2011-S.O. no. 54; Libreria dello Stato: Rome, Italy, 2011. (In Italian)
77. Lagomarsino, S.; Cattari, S.; Ottonelli, D.; Giovinazzi, S. Earthquake damage assessment of masonry churches: Proposal for rapid and detailed forms and derivation of empirical vulnerability curves. *Bull. Earthq. Eng.* **2019**, *17*, 3327–3364. [CrossRef]
78. De Matteis, G.; Mazzolani, F.M. The Fossanova Church: Seismic vulnerability assessment by numeric and physical testing. *Int. J. Archit. Herit.* **2010**, *4*, 222–245. [CrossRef]
79. INGV. Gruppo di Lavoro sul Terremoto in Centro Italia. Rapporto di Sintesi sul Terremoto in Centro Italia Mw 6.5 del 30 Ottobre 2016. Available online: https://zenodo.org/record/166019#.YEJT12hKhPY (accessed on 5 March 2021).
80. ITACA–ITalian ACcelerometric Archive. Available online: http://itaca.mi.ingv.it/ItacaNet_31/#/event/search (accessed on 5 March 2021).
81. Direttiva del Presidente Consiglio dei Ministri (DPCM) del 13 Marzo 2013. Approvazione del Manuale per Compilare la Scheda di Rilievo del Danno ai Beni Culturali. Available online: https://www.protezionecivile.gov.it/it/normativa/dpcm-del-13-marzo-2013 (accessed on 5 March 2021).
82. Galli, P.; Castenetto, S.; Peronace, E. Rapporto sugli effetti macrosismici del terremoto del 30 Ottobre 2016 (Monti Sibillini) in scala MCS. *Roma Rapp. Congiunto DPC CNR-IGAG* **2017**, *17*, 8.
83. Istituto Nazionale di Geofisica e Vulcanologia. Available online: http://shakemap.rm.ingv.it/shake/archive/2016.html (accessed on 5 March 2021).
84. Marotta, A.; Sorrentino, L.; Liberatore, D.; Ingham, J.M. Seismic risk assessment of New Zealand unreinforced masonry churches using statistical procedures. *Int. J. Archit. Herit.* **2018**, *12*, 448–464. [CrossRef]